Experiments on Smoke Behavior in Cavity Spaces Part 2 The case of a cavity space with an opening at the bottom

TERUHISA FUKUDA
Shimizu Corporation
Seavans South No. 2-3
Shibaura 1-chome, Minato-ku, Tokyo 105-07, Japan

TAKEYOSHI TANAKA
Building Research Institute
Ministry of Construction
1 Tatehara, Tsukuba-shi, Ibaraki-ken, 305 Japan

TAKAO WAKAMATSU
Science University of Tokyo
2461 Yamasaki, Noda-shi, Chiba-ken, 278 Japan

ABSTRACT

It has been demonstrated by previous experiments within a cavity space having no bottom opening that the temperature rise of a plume at the height of the cavity opening is well scaled by a nondimensional temperature defined as $\Theta \equiv \left(\overline{\Delta T} / T_\infty\right) / \dot{Q}^{*2/3}$ where $\dot{Q}^* \equiv \dot{Q} / \rho_\infty C_p T_\infty \sqrt{g} D D^2$, and the temperature is successfully correlated as $\Theta = \alpha (H/D)^\beta$, where β= -5/3, -1 and -1/3 for shallow, intermediate and deep cavities[1),2)], respectively.

In this study, the smoke behavior in cavity spaces is further investigated by small scale experiments for a cavity space which has an opening at the bottom. It is shown that as the area of the bottom opening becomes larger, the fire plume becomes more stable, but the temperature is still well correlated in the same manner as for a cavity having no bottom opening. The effects of a bottom opening on the temperature and the pressure difference produced in the cavity are also analyzed.

KEYWORDS: smoke behavior, cavity space, fire plume, bottom opening, plume temperature, pressure difference, air inflow rate

1. INTRODUCTION

The primary fire safety issue concerning cavity spaces in buildings is the potential hazard that such spaces may become a dominant passage for smoke spread throughout the buildings. A means to predict smoke behavior in cavity spaces is necessary to allow development of rational measures for evacuation safety in the buildings having such cavity-like spaces.

In previous papers[1),2)], formulas for predicting the temperature of plumes as a function of fire heat release rate and cavity dimensions were obtained for cases where no opening exists at the bottom of the space. On the other hand, some cavity spaces in buildings have openings near the bottom. In Japan, building officials and fire department suspect that air supplied through such openings contributes to the mitigation of smoke hazard, and tend to insist on providing an opening for the cavity space when it exceeds a certain depth. However,

virtually no solid data is available for assessing how effective the openings are or how large they should be. While all of the air entrained into a fire plume is supplied through the opening at the top for the case of a cavity having no bottom opening, the air will be supplied both from the top and the bottom in case of a cavity having an opening at the bottom. The portion of the air supplied at the bottom may increase as the area of the bottom opening increases. Consequently, the existence of an opening at the bottom may significantly affect the smoke behavior in a cavity. In this study, reduced-scale experiments are conducted for cases where an opening exists at the bottom of a cavity, and the effects of the bottom opening size on the plume temperature and the pressure profile in the cavity are investigated.

2. EXPERIMENTAL SETUP

The cavity space model used in this experiment is the same as in an earlier experiment[1]. It has a square floor of 0.8 m x 0.8 m whose height can be changed from 0 m to 3 m using wires and a pulley. The tests are carried out for depths of the cavity which increase from 0.25 m to 3.0 m in steps of 0.25 m.

A 7 cm diameter diffusion flame burner is used as the fire source with heat release rates set to 0.5, 1.0, 2.0, 3.0 and 4.0 kW by adjusting the rate of supply of methane. The fire source is set on the center of the floor, as shown in FIGURE 1.

The bottom opening in each test is arranged on the floor uniformly around the fire source as shown in Figure 1 in order to maintain as symmetric conditions as possible and also to avoid the brown down of flames due to the draft induced through the opening. The areas of the opening used are 0.03, 0.067 or 0.163 m^2 .
The measurements recorded are also the same as in Ref.[1]; 85 thermocouples are spaced uniformly over the opening at the top of the space to measure the temperatures of the gases flowing out of and the air flowing into the space; Pressure measurements probes arranged at 10 locations on the rear wall provide pressure difference between the inside and outside of the cavity space. Data acquisition is started 15 minutes after the ignition of the fire source and data recording is carried out for 5 minutes at 5 second intervals.

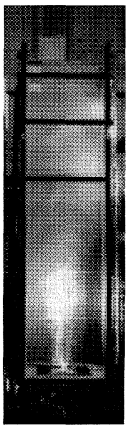

Fire plume in the cavity

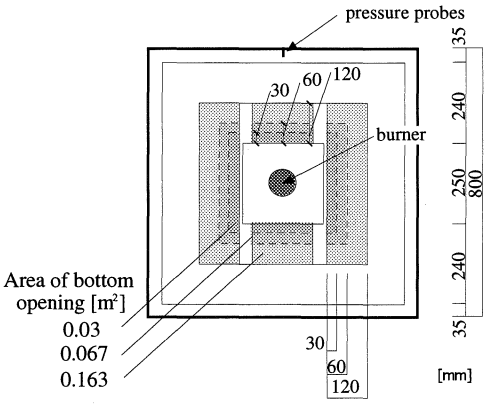

Cavity floor plan

FIGURE 1 Cavity Space Model and Arrangement of Bottom Opening

3. RESULTS OF THE EXPERIMENTS

3.1 Temperature Profiles at the Top Opening

FIGURE 2 compares typical temperature profiles at the opening at the top of the cavity using different areas for the bottom opening. The heat release rate of the source for the examples in Figure 2 is 2.0 kW, and the cavity depth is either 0.5 m or 3.0 m.

As can be seen from the figures for H=0.5 m, the larger the area of the bottom opening, the more sharply peaked the temperature profile, for the small cavity depth. On the other hand, temperature profiles tend to become less sharp with increasing the bottom opening area when the cavity depth is large.

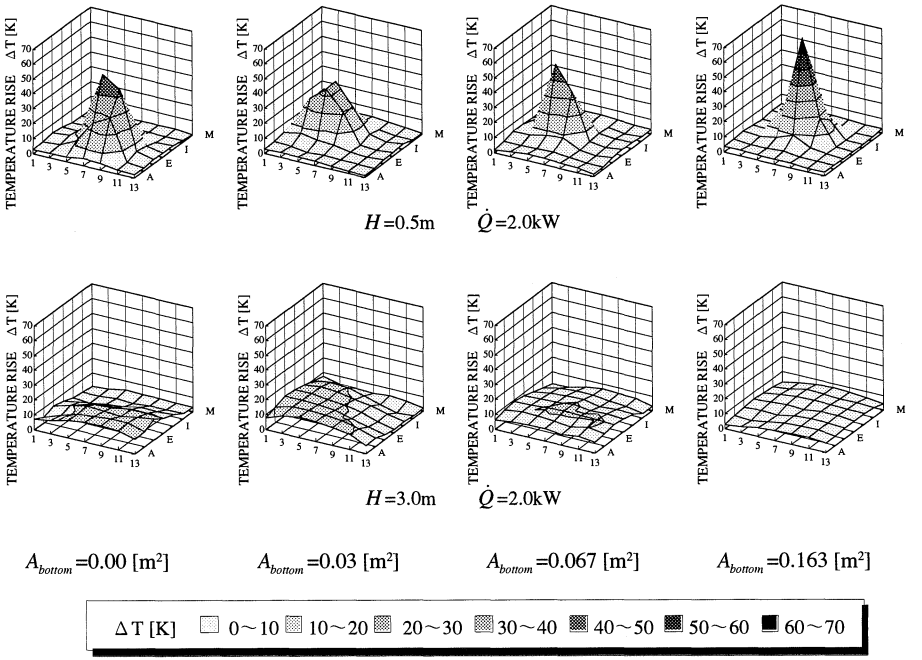

FIGURE 2 Temperature Profile at Top Opening

3.2 Plume Axis Location Fluctuation

FIGURE 3 shows examples of the observed spatial distributions for the highest temperature measured by the 85 thermocouples arrayed across the cavity opening for the 60 measurements recorded during the 5 minutes of data acquisition. The examples are taken from the cases where the heat release rate was 2.0 kW and cavity depths were 1.0 m and 2.0 m.

Here we assume that the plume axis exists at the position where the highest temperature is recorded. It can be seen from FIGURE 3 that increasing of the area of the bottom opening stabilizes the location of the fire plume. This effect is particularly remarkable when the cavity depth is large, but still apparent when the cavity depth is small.

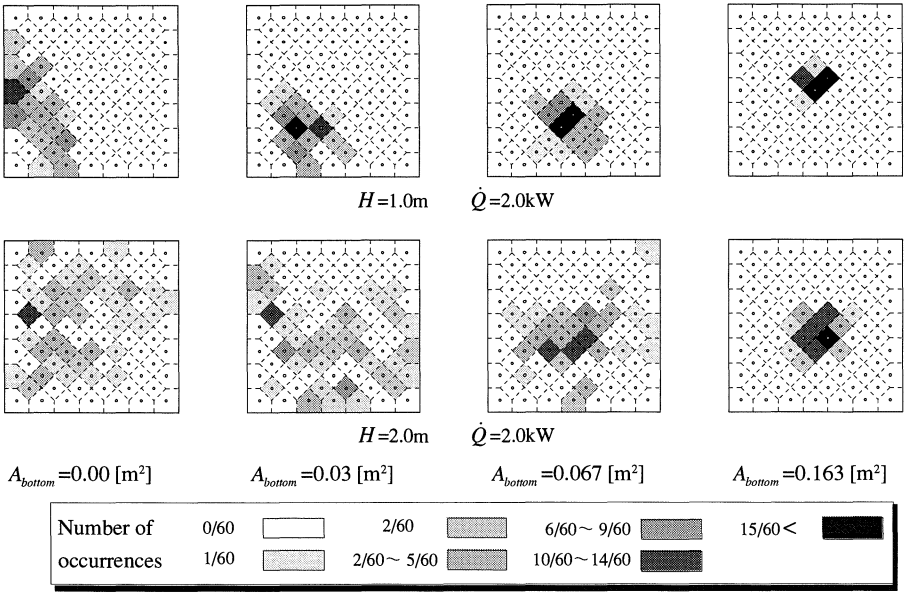

FIGURE 3 Plume Axis Location Fluctuation
(Highest temperature measured at the cavity opening for the 60 recordings during 5minutes)

3.3 Pressure Difference Vertical Profiles

Figure 4 shows vertical profiles for the pressure differences which develop between the inside and the outside of the 3.0 m deep cavity space. Each value of the pressure difference is the average of the 60 measurements recorded during each test. The pressure differences are nearly zero or slightly negative at the height of the cavity opening and increase roughly proportionally to the distance from the opening, but the increases seem to be nonlinear with height near the middle height of the cavity.

The pressure differences increase with the heat release rate when the area of the bottom opening is the same, and decrease as the bottom opening area increases if the heat release rate is held constant.

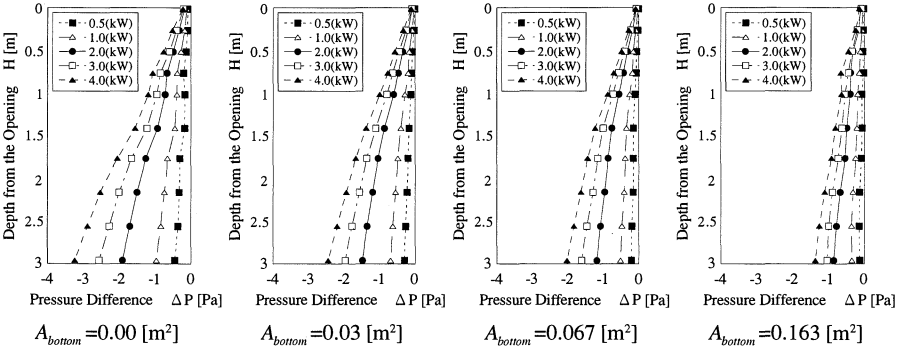

FIGURE 4 Pressure Difference Vertical Profiles in the 3.0m Deep Cavity Space

3.4 Plume Area

The proportion of the plume horizontal area at the height of the opening of the cavity to the floor area of the cavity (plume area ratio) is plotted versus the depth of the cavity in FIGURE 5. The plume area was calculated as the area of the opening in which the thermocouple readings obeyed the following condition:

$$\Delta T \geq (T_{\max} - T_{\infty}) \times k \tag{1}$$

with k=0.25, where $T_{\max}$, T_{∞} and ΔT are the highest temperature reading observed by the thermocouples, the ambient air temperature and the temperature difference of a thermocouple reading and ambient air, respectively.

Similar to the previous findings for a cavity space having no opening at the bottom, the plume area does not depend on heat release rate and tends to increase with cavity depth H approximately in proportional to H^2, H^1 and H^0 when the depth is small, intermediate and large, respectively. The plume area ratio for large cavity depth tends to increase with the area of the opening at the bottom, but the cavity depth at which the transition from intermediate to deep behavior takes place seems to increase.

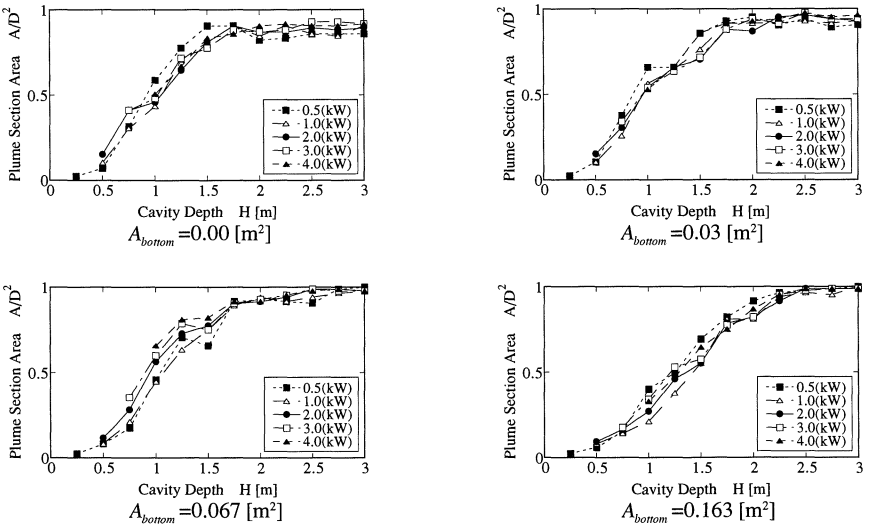

FIGURE 5 Nondimensional Plume Area A/D² at Cavity Opening

3.5 Average Temperature Rise of the Fire Plume Area

The average temperature within the plume area defined by Eqn.(1) with k=0.25 is plotted versus the depth of the cavity in FIGURE 6. Each value of the temperature in the figure is the average of 60 average plume temperature measurements obtained during the 5 minutes of data acquisition. Each individual average is obtained by averaging the temperature within the instantaneous plume area defined by Eqn.(4).

A similar tendency is observed in the temperature rise regardless of the size of the open area at the bottom as shown in FIGURE 6. The temperature falls significantly with cavity depth while the depth is small, but it changes only slightly when the depth is large. The larger the opening area at the bottom is, the lower the temperature is for a large depth as long as the heat release rate is constant.

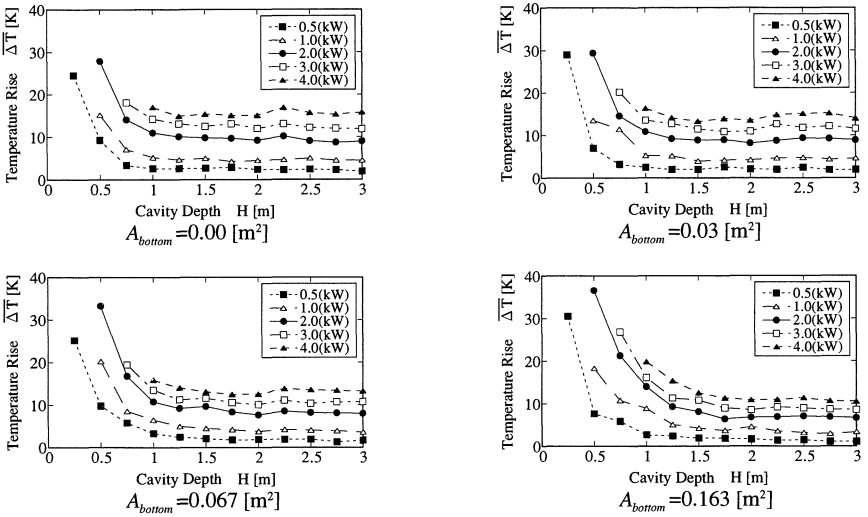

FIGURE 6 Temperature Rise at Top Opening with different Depth and Heat Release Rate

4. EQUATIONS FOR PLUME TEMPERATURE

In our earlier work[1),2)], it was theoretically predicted and experimentally verified for the cavity closed at the bottom that the temperature of a fire plume in a cavity space can be well correlated as

$$\Theta = \alpha(H/D)^{\beta} \tag{2}$$

where β is - 5/3, -1 and -1/3 for shallow, intermediate and deep cavities, respectively (See NOTE). Θ is the nondimensional temperature defined as

$$\Theta \equiv \left(\overline{\Delta T}/T_{\infty}\right)/\dot{Q}^{*2/3} \tag{3}$$

and $\dot{Q}^{*}$ is the nondimensional heat release rate defined as

$$\dot{Q}^{*} \equiv \dot{Q}/\rho_{\infty}C_{P}T_{\infty}\sqrt{gD}D^{2} \tag{4}$$

Since it is believed that essentially the same theoretical considerations should apply for cavities opening at the bottom, the equations for correlating plume temperatures are derived using the same relationships as in Eqns.(2) -(4).

4.1 Equations for Plume Average Temperature

The plume average temperatures are nondimensionalized in the form of Eqn.(2) and plotted versus H/D as shown in FIGURE 7. It can be seen that the data in FIGURE 6, which vary depending on heat release rate, are successfully collapsed to single lines. The solid and the broken lines in the figures indicate the results when the theoretical and the results of a regression analysis for the experimental values are employed for β in Eqn.(2). Values for α and β from the theoretical and experimental regression results are summarized in TABLE 1. Note, however, that α cannot be theoretically obtained for either case. The values of α for the "Theory" are in reality chosen from the experimental values to best fit the test data when the theoretical β is used. Since there is no meaningful difference in the accuracy using either value for β, as can be seen from the

insignificant difference between the solid and broken lines FIGURE 7, the equations using the theoretical β should be sufficient for predicting the plume average temperature.

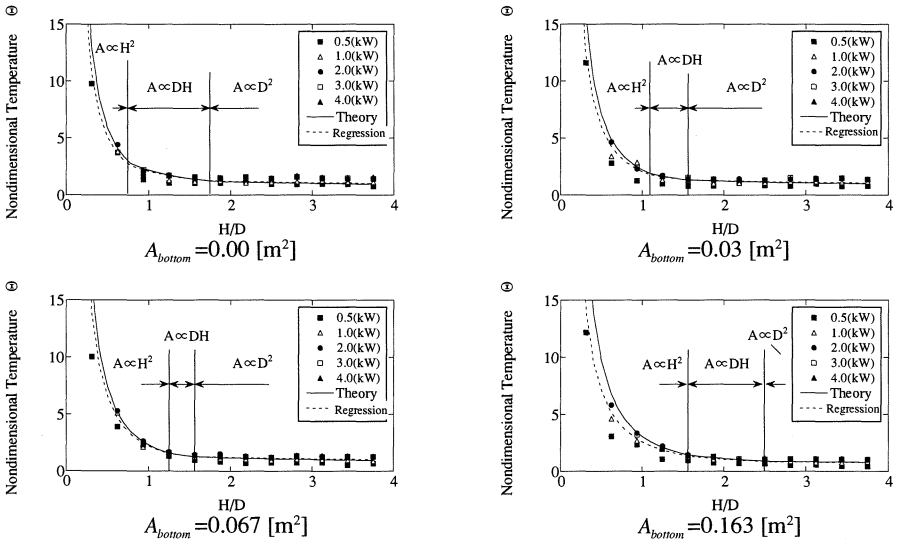

FIGURE 7 Nondimensional Temperature as A Function of Nondimensional Cavity Depth and Open Area at the Bottom of Cavity

TABLE 1 Comparion of α and β for regression analysis of theoretical and experimental expression

Opening Area [m²]	Region	Regression		Theory	
		α	β	α *)	β
0.00	H/D≦0.78	1.74	-1.55	1.86	-5/3
	0.78<H/D≦1.77	2.09	-0.90	2.19	-1
	1.77<H/D	1.48	-0.28	1.48	-1/3
0.03	H/D≦1.09	2.07	-1.53	2.23	-5/3
	1.09<H/D≦1.56	1.93	-0.81	2.09	-1
	1.56<H/D	1.51	-0.26	1.56	-1/3
0.0672	H/D≦1.25	2.23	-1.56	2.33	-5/3
	1.25<H/D≦1.56	1.91	-0.86	2.01	-1
	1.56<H/D	1.45	-0.26	1.49	-1/3
0.1632	H/D≦1.56	2.60	-1.45	3.08	-5/3
	1.56<H/D≦2.50	2.07	-0.93	2.29	-1
	2.50<H/D	1.16	-0.30	1.24	-1/3

*) Experimental value to best fit the test data when theoretical β is used

4.2 Dependence of Plume Temperature for Large Depth Opening Area at the Bottom

It is believed that the smoke hazard in cavity spaces is particularly serious for deep cavities. When H / D is small contamination by smoke will be confined to a limited part of the space in a manner similar to a window jet to the outside. However, when H / D is large the space can be extensively exposed to the influence of the smoke.

As can be seen from the values of the coefficient α for large H/D in TABLE 1, the temperatures for large depth decrease with the increase of the opening area at the bottom, thus indicate an opening may help mitigate the smoke hazard. Here we characterize the effect using the opening ratio γ which is defined as the ratio of opening area at the bottom to the horizontal cross sectional area of the cavity, i.e.,

$$\gamma \equiv A_{bottom} / D^2 \tag{5}$$

The reason why the temperature for large depths decreases with the increase of the open area at the bottom is believed to be because the rate of the air supply through the opening at the top of the cavity space decreases as the open area at the bottom increases, so more fresh air is entrained into the fire plume. Nevertheless, the air supplied from the top of the cavity has a significant effect on diluting the fire plume gases even when A_{bottom} is zero. Since it is considered that both the air supply from the top and the bottom have significant effects on the temperatures, the values of the coefficient α for large H/D are plotted in FIGURE 8 versus

$$\frac{A_{bottom} + D^2}{D^2} = \gamma + 1 \tag{6}$$

instead of simply plotting versus γ. Note that the value of for γ=0 (no bottom opening) is taken from earlier work [3]. The experimental correlation between α and γ is given by

$$\alpha = 1.67(\gamma + 1)^{-4/3} \tag{7}$$

Note, however, that an inconsistency in the value for γ=0 compared to the regression curve has been ignored.

Substituting Eqn.(7) into Eqn.(2) yields the generalized formula for the average plume temperature for large H/D as:

$$\Theta = 1.67(\gamma + 1)^{-4/3}(H/D)^{-1/3} \tag{8}$$

Eqn.(8) should be applied conservatively to cases with $0 < \gamma < 0.25$ since its applicability outside these limits has not been tested either experimentally nor theoretically. However, based on the area ratios of existing cavity spaces with openings at the bottom, this limit on the application of Eqn.(8) is not a severe limitation.

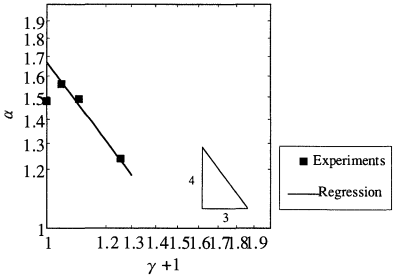

FIGURE 8 α as a Function of Bottom Opening Area Ratio

5. PRESSURE DIFFERENCE

5.1 Nondimensional Pressure Difference

The pressure difference which develops between the inside and the outside of a cavity space affects the measures required for protecting floor areas adjacent to the cavity space from the infiltration of smoke.

According to FIGURE 4, which shows the pressure difference profile for the cavity with a 3 m depth, the pressure difference is nearly zero at the height of the top opening regardless of variations in heat release rate and the open area at the bottom, but the profile depends on the conditions.

Although the exact mechanism for the pressure development is not obvious, since the pressure difference increases with the distance from the top, at least down to the middle of the cavity, the pressure difference at the bottom ΔP_{bottom} may be assumed to be given by

$$\Delta P_{bottom} \propto \Delta \rho g H \tag{9}$$

Dividing both sides of Eqn.(9) by $\Delta \rho_\infty g H$ and noting that for large H / D the relationship

$$\frac{\Delta T}{T_\infty} \propto \dot{Q}^{*2/3} \left(\frac{H}{D} \right)^{-1/3}$$

is valid, we have

$$\frac{\Delta P_{bottom}}{\rho_\infty g H} \propto \frac{\Delta \rho}{\rho_\infty} \approx \frac{\Delta T}{T_\infty} \propto \dot{Q}^{*2/3} \left(\frac{H}{D} \right)$$

However, this assumption may fail because the temperature in the lower part of a cavity space cannot be represented by the plume temperature. Hence, based on the above considerations, we will introduce a nondimensional pressure π defined as

$$\pi \equiv \left(\Delta P_{bottom} / \rho_\infty g H \right) / \dot{Q}^{*2/3} \tag{10}$$

and investigate the dependence of π on cavity depth.

In FIGURE 9, the nondimensional pressure π for cavities having different depths are plotted versus H / D. According to FIGURE 9, the data for 2.0, 3.0 and 4.0kW fires collapse to a single line for each opening area, which implies that the pressure difference is scaled well by π. Although the data for 0.5 and 2.0 kW fire are not necessarily in good agreement, this is thought to be due to the fire sizes being too small to induce large enough pressure difference for accurate measurement.

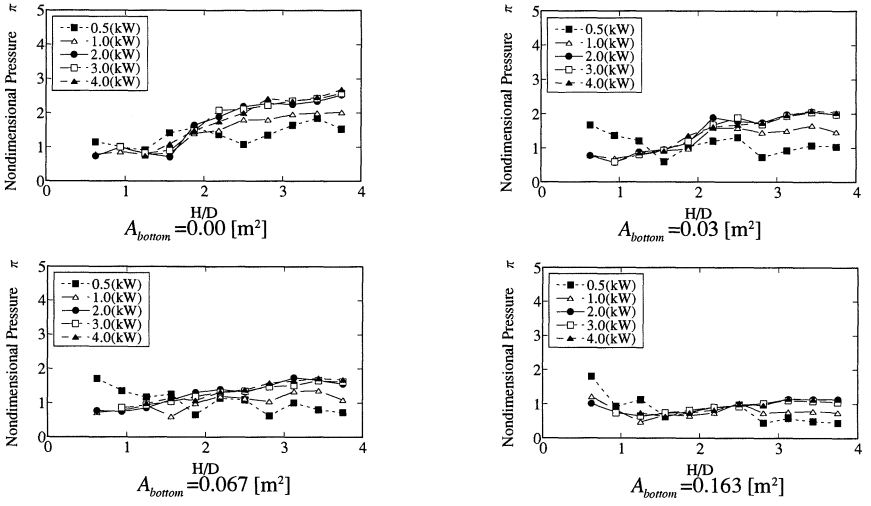

FIGURE 9 Nondimensional Pressure in Cavities with Different Nondimensional Depth

5.2 Dependence of Pressure Difference on Open Area at the Bottom

Looking at FIGURE 9, π is nearly constant when H/D is large and proportional to H/D when H/D is intermediate, while a consistent behavior cannot be observed when H/D is small. In order to investigate the dependence of the pressure difference on the open area at the bottom, π for cavity spaces with large H/D and 2.0, 3.0 and 4.0 kW fires are plotted versus $\gamma+1$ in FIGURE 10. Regression line analysis of the results gives

$$\pi = 2.3(\gamma+1)^{-10/3} \tag{11}$$

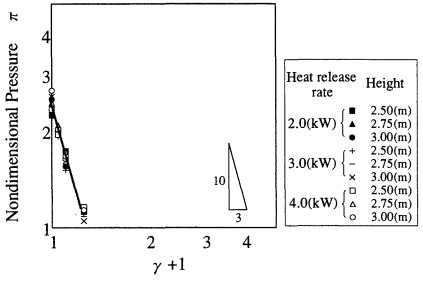

FIGURE 10 Nondimensional Pressure as a Function of Bottom Opening Area Ratio

From FIGURE 9, the boundary between intermediate and large depth seems to lie somewhere near H/D=2.5, we will assume that Eqn.(11) applies for H/D>2.5. Then, in case cavity depth is H/D<2.5, noting that π increases nearly proportionally to H/D, π may be written as

$$\pi = 0.92(\gamma+1)^{-10/3}(H/D) \tag{12}$$

From FIGURE 11, which compares the experimental data and Eqns.(11) and (12), Eqn.(12) is found to be applicable roughly for H/D <2.5. Incidentally, Eqns.(11) and (12) should be considered to be only applicable for 0< γ <0.25.

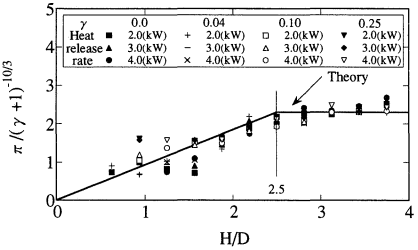

FIGURE 11 $\pi/(\gamma+1)^{-10/3}$ v.s. H/D

6. RATE OF AIR INFLOW THROUGH BOTTOM OPENING

The rate of air inflow through the opening at the bottom m_{bottom} is given by

$$m_{bottom} = C_D A_{bottom}\sqrt{2\rho_\infty \Delta P_{bottom}} \tag{13}$$

Substituting Eqn.(10) into Eqn.(13), we have

$$m_{bottom} = C_D \rho_\infty A_{bottom}\sqrt{2gH\pi}\dot{Q}^{*1/3} \tag{14}$$

Introducing a nondimensional flow rate defined as

$$\mu \equiv \left(m_{bottom} / \rho_\infty \sqrt{gD^5}\right) / \dot{Q}^{*1/3} \tag{15}$$

and substituting this into Eqn.(14) gives

$$\mu = C_D \sqrt{2}\left(A_{bottom} / D^2\right)\pi^{1/2}(H/D)^{1/2} = C_D \sqrt{2}\gamma\pi^{1/2}(H/D)^{1/2} \tag{16}$$

Using Eqns.(11) and (12), and setting C_D=0.7, we obtain

$$\mu = \begin{cases} 0.95\dfrac{\gamma}{(\gamma+1)^{5/3}}\left(\dfrac{H}{D}\right) & (H/D < 2.5) \\ 1.50\dfrac{\gamma}{(\gamma+1)^{5/3}}\left(\dfrac{H}{D}\right)^{1/2} & (2.5 \le H/D) \end{cases} \tag{17}$$

Figure 12 shows a comparison of Eqn.(17) with the nondimensional air inflow rates from measurements. Notice that the latter is calculated using the pressure difference measured at the bottom of the cavity. Hence the comparison of air inflow rates in Figure 12 is simply different form of comparison of pressure differences shown in FIGURE 11, although the data for no bottom opening are naturally omitted. Eqn.(17) will be convenient to estimate flow rate of air through opening directly.

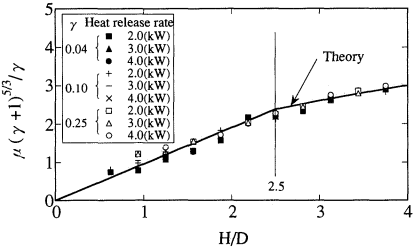

FIGURE 12 $\mu(\gamma+1)^{5/3}/\gamma$ v.s. H/D

7. CONCLUDING REMARKS

Experiments have been conducted for elucidating the behaviors of fire plumes in cavities which have openings at the bottom. It was found that the larger the opening at the bottom, the more stable the fire plume becomes, but that the temperature is still correlated in the same manner as for the case of cavity with no opening at the bottom.

The effects of the opening area at the bottom on the plume temperature, the pressure difference induced in the cavity space and the mass inflow rate of air through the bottom opening are investigated and experimental correlations are given.

NOTE : Derivation of Relationship between nondimensional temperature and height

The heat transported by the plume convection is expected to be proportional to the heat release rate, i.e.,

$$\dot{Q} \propto \rho C_P \overline{\Delta T} A \bar{u} \tag{N1}$$

where ρ, $\overline{\Delta T}$ and $\bar{u}$ are the average density, temperature rise and flow velocity of plume at a given height, respectively and A is the plume horizontal section area.

The plume average velocity $\overline{u}$ is caused by buoyancy, so

$$\rho\overline{u}^2 \propto \overline{\Delta\rho} g H \tag{N2}$$

where $\overline{\Delta\rho}$ is the average density difference between the ambient air and the plume, and H is the representative height, Using Eqns.(N1) and (N2) yields

$$\overline{\Delta T}^{3/2} \propto \frac{\dot{Q} / \rho C_P}{\sqrt{g / T} A H^{1/2}} \tag{N3}$$

The plume sectional area A in a cavity space is expected to be

$$A \propto \begin{cases} H^2 & (H << D) \\ DH & (H \approx D) \\ D^2 & (D << H) \end{cases} \tag{N4}$$

where D is the representative side length of cavity. Substituting Eqn.(N4) into (N3) yield:

$$\Theta \propto \begin{cases} (H/D)^{-5/3} & (H << D) \\ (H/D)^{-1} & (H \approx D) \\ (H/D)^{-1/3} & (D << H) \end{cases} \tag{N5}$$

where Θ is the nondimensional temperature defined by Eqn.(3) in the text.

NOMENCLATURE

A	Horizontal section area of fire plume (m^2)
A_{bottom}	Area of bottom opening (m^2)
C_P	Specific heat of air (kJ/kgK)
C_D	Flow Coefficient
D	Length of the side of cavity space (m)
g	Acceleration due to gravity (m/s^2)
H	Depth of cavity (m)
m_{bottom}	Rate of air inflow through bottom opening (kg/s)
γ	Ratio of area of opening at the bottom to cavity cross sectional area
ΔP	Pressure difference (Pa)
ΔP_{bottom}	Pressure difference at the bottom of cavity space (Pa)
$\dot{Q}$	Heat release rate of fire source (kW)
$\dot{Q}^*$	Nondimensional heat release rate defined by Egn.(4)
T	Temperature (K)
T_∞	Ambient temperature (K)
ΔT	Temperature difference (K)
α	Coefficient of Eqn.(2)
β	Factor of Eqn.(2)
ρ_∞	Ambient air density (kg/m^3)
π	Nondimensional pressure defined by Eqn.(10)
μ	Nondimensional flow rate defined by Eqn.(15)
Θ	Nondimensional temperature defined by Eqn.(3)

REFERENCES

[1] Takeyoshi TANAKA and Sunao KUMAI, Experiments on Smoke Behavior in Cavity Spaces, Fire Safety Science, Fourth Int'l Symp., 1994

[2] Takeyoshi TANAKA, Sunao KUMAI, Teruhisa FUKUDA, Akihiko YOSHIZAWA, Osamu ISHINO and Takao WAKAMATSU, Smoke Behavior in Cavity Spaces, Part 1 In case where the fire sources are located at the center of the cavity floor, Transaction of AIJ, No.469,1995

[3] Teruhisa FUKUDA, Akihiko YOSHIZAWA, Sunao KUMAI, Osamu ISHINO, Takeyoshi TANAKA and Takao WAKAMATSU, Smoke Behavior in Cavity Spaces, Part 2 In case where the fire sources are located by a wall or at a corner, Transaction of AIJ, No.478,1995